Proc. of SPIE Vol. 1998, Optomechanical Design, ed. D Vukobratovich, P R Yoder, V L Genberg (Sep 1993) Copyright SPIE

Parametric investigations of mounting-induced axial contact stresses in individual lens elements

Paul R. Yoder, Jr.

Consultant in Optical Engineering, 1220 Foxboro Drive, Norwalk, CT 06851

ABSTRACT

Analytical techniques for estimating the axial contact stress in a single element lens mechanically clamped near its rim have previously been described.[1,2] In this paper, we present a progress report on an ongoing investigation of the effects upon this stress of changing the interface type, the geometric parameters and dimensions of the design or the materials used. The sensitivity of the design to temperature changes also is discussed. From the trends shown here, the optomechanical engineer can predict approximately what consequences might be expected if various parameters are changed during the design phase.

1. INTRODUCTION AND THEORETICAL BACKGROUND

Analytical techniques for estimating the axial contact stress in a lens mechanically clamped near its rim by means such as a threaded retaining ring (see Fig. 1) as well as the variation of the clamping force due to temperature changes have previously been described.[1,2] In this section, we summarize the key equations used in these techniques for the convenience of the reader.

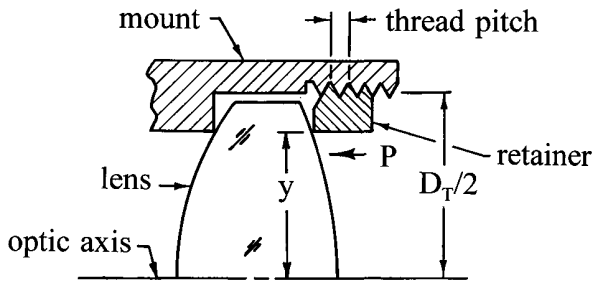

Fig. 1 - Schematic of a lens element clamped axially by a threaded retaining ring.

The axial preload, P, applied over a very narrow annular region on the lens surface at a fixed temperature can be estimated approximately from the torque applied to the retainer from the equation:

$$P = 5 \text{ (torque)}/DT \tag{1}$$

where D_T is the pitch diameter of the thread.

Within an annular region centered at the height of mechanical contact and of radial width equal to the edge thickness of the lens element at that height, the peak axial stress, S_A , can be estimated by the following equation adapted from Roark[3]:

$$S_A = 0.798 \, (K_1 \, p \, / \, K_2)^{1/2} \tag{2}$$

where K_1 depends upon the interface design and lens surface radius, K_2 depends upon the material properties and p is the linear preload as given by:

$$p = P/2\pi y. \tag{3}$$

Here, y is the height of contact on the surface.

For a "sharp corner" interface of the types shown schematically in Fig. 2 or a toroidal (donut) interface of the types shown in Figs 3 and 4, the value of K_1 is given by:

$$K_1 = (D_1 \pm D_2)/D_1D_2 \tag{4}$$

where D_1 = 2(surface radius) and D_2 = 2(corner radius). The "+" sign applies to convex surfaces while the "-" sign is used with concave surfaces. For the "sharp corner" interface only, D_2 can be assumed constant at 0.004 in. (0.1 mm).[4] Then K_1 would be constant at approximately 250/in. (10/mm) for all surface radii larger than 0.2 in. (5.1 mm).

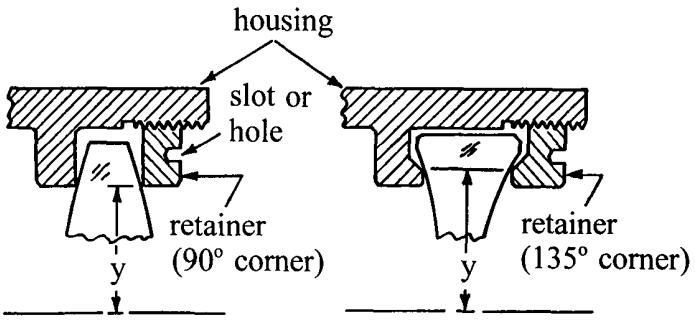

Fig. 2 - Schematics of "sharp corner" interfaces on convex and concave surfaces.

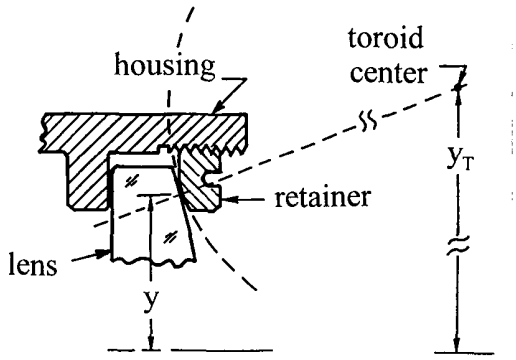

Fig. 3 - Schematic of a toroidal (donut) interface on a convex surface.

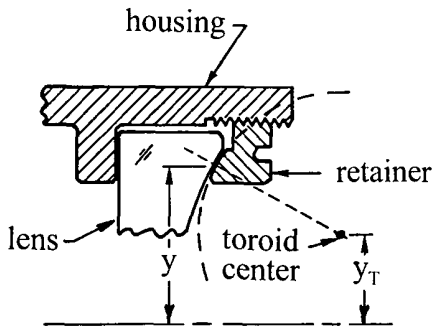

Fig. 4 - Schematic of a toroidal (donut) on a concave surface.

As pointed out previously[5], "preferred" values for the radii of toroidal contacts on a lens surface of radius, R, are -10R for a convex surface and +0.5R for a concave surface. Then,

$$K_1 = 1.1/D_1 = -0.55/R \quad \text{(for convex surfaces)} \tag{5}$$

and

$$K_1 = 1/D_1 = +0.5/R \quad \text{(for concave surfaces)} \tag{6}$$

For a tangent (conical) interface of the type shown in Fig. 5,

$$K_1 = 1/D_1 = 0.5/R. \quad (7)$$

It should be noted that a tangent interface is feasible only with a convex lens surface.

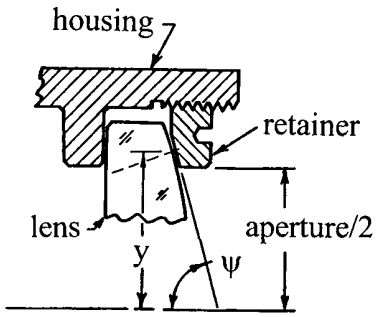

Fig. 5 - Schematic of a tangential interface on a convex surface.

For all interface types, the term K_2 in Equation (2) is given by:

$$K_2 = [(1 - \upsilon_G^2)/E_G] + [(1 - \upsilon_M^2)/E_M] \quad (8)$$

where υ_G , E_G, υ_M and E_M are Poisson's ratio and Young's modulus for glass and metal respectively.

If, as is usually the case, the lens and mount materials have dissimilar thermal expansion coefficients, temperature changes cause changes in axial preload exerted onto the lens. The following equation quantifies this relationship:

$$\Delta P = K_3(\Delta T) \quad (9)$$

where $K_3 = -E_G A_G E_M A_M(\alpha_M - \alpha_G)/(2)((E_G A_G/2) + E_M A_M)$ (10)

Here, α_M and α_G are the thermal expansion coefficients of the mount and lens respectively and ΔT is the temperature change. To determine A_G and A_M , we proceed as follows. If t_E is the edge thickness of the lens at the contact height y, t_C is the radial wall thickness of the mount, D_M is the inside diameter of the mount at the lens rim and D_G is the outside diameter of the lens, then

$$A_G = 2\pi y t_E \quad \text{if } 2y + t_E < D_G \quad (11)$$

or

$$= (\pi/4)(D_G - t_E + 2y)(D_G + t_E - 2y) \quad \text{if } 2y + t_E >= D_G \quad (12)$$

$$A_M = 2\pi t_C((D_M/2) + (t_C/2)). \quad (13)$$

2. STRESS VARIATION WITH INTERFACE TYPE

Figure 6 shows the nature of the variation of axial stress with radius of the contacting corner for a particular design having constant convex lens surface radius and constant mechanical preload. Both stress and corner radius are plotted logarithmically to cover large ranges of variability. At the left, we find the short corner radius characteristic of the "sharp corner" interface while at the right we approach asymptotically to the tangential interface case. Between these extremes are an infinite number of toroidal interface designs. The "preferred" toroidal radius (equal to -10R) for which the stress is within 5 percent of the tangential value is indicated by the circle.

Figure 7 shows a similar relationship for a concave lens surface example. The "sharp corner"

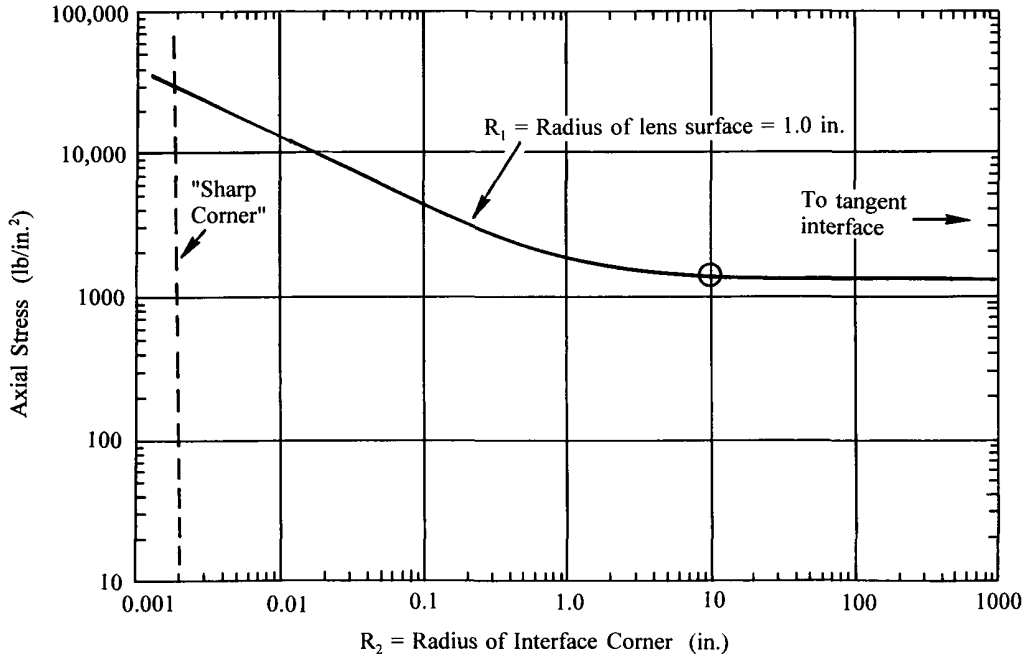

Fig. 6 - Variation of axial stress in a typical lens as the radius of the mechanical surface contacting its convex surface is changed.

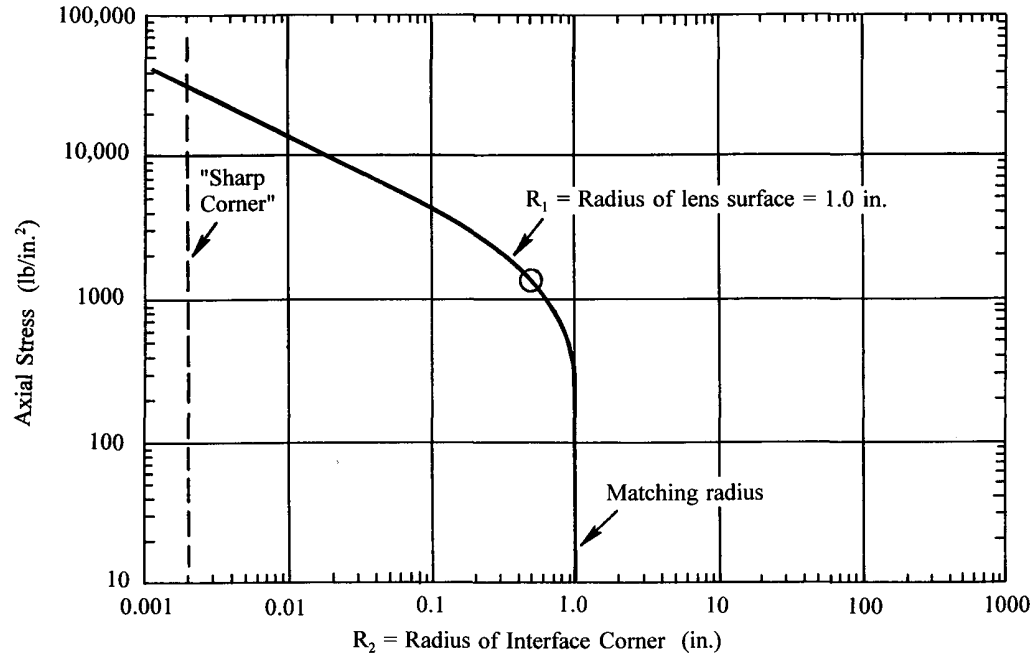

Fig. 7 - Variation of axial stress in a typical lens as the radius of the mechanical surface contacting its concave surface is changed.

case is again at the left. As the toroidal radius increases towards the matching radius limit, the stress decreases. The circle represents the "preferred" toroidal radius of +0.5R for which the stress approximates that which would prevail at the same preload on a convex surface of the same radius.

Since the contact stress is always significantly higher with a "sharp corner" interface, we are led to recommend that, whenever slightly higher manufacturing cost can be tolerated, tangential interfaces be used on all convex lens surfaces and toroidal interfaces of radius approximately +0.5R be used on all concave surfaces.

3. STRESS VARIATION WITH SURFACE RADIUS

Figure 8 shows graphically how the axial stress varies as the surface radius is changed by successive factors of 10 for convex surface cases. The stress is independent of surface radius or its algebraic sign for a "sharp corner" interface. The greatest change occurs for long-radii toroids and for the tangential interface cases. Algebraic manipulation of Equation (4) for the special (preferred) case where the toroidal radius equals -1.1R reveals that if the surface radius changes from R1 to R2 with all other parameters unchanged, the corresponding stress changes by $(R1/R2)^{1/2}$. Hence, for the 10:1 increases in surface radius depicted in Fig. 8, the stress decreases by a factor of $0.1^{1/2} = 0.316$.

Similarly, Fig. 9 shows variations in the axial stress with 10-fold changes in concave surface radius. With all other parameters constant, the stress dependence upon surface radius for the preferred +0.5R toroidal radius case is again $(R1/R2)^{1/2}$ so each 10:1 radius increase reduces the stress by a factor of 0.316.

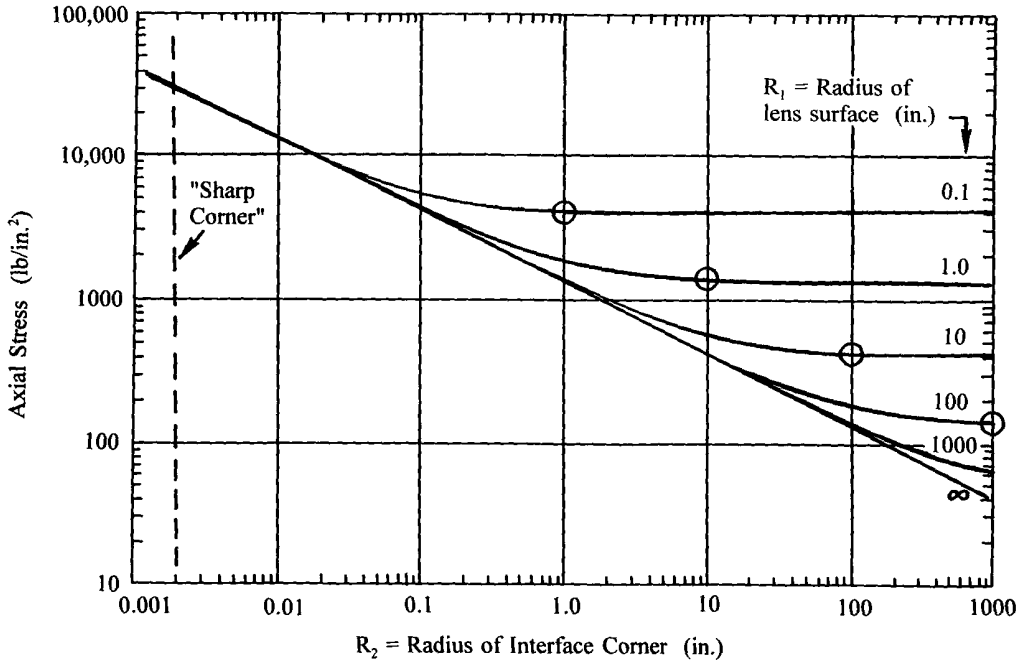

Fig. 8 - Variations of axial stress in a family of typical lenses as the radius of the mechanical surface contacting its convex surface and the radius of that surface are changed.

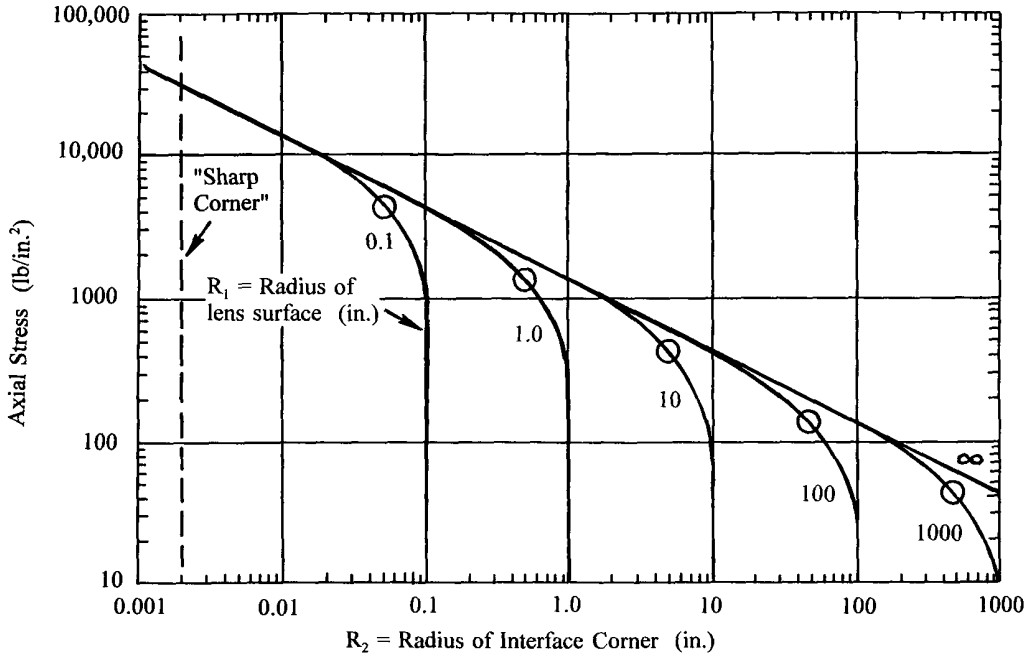

Fig. 9 - Variations of axial stress in a family of typical lenses as the radius of the mechanical surface contacting its concave surface and the radius of that surface are changed.

4. STRESS VARIATION WITH PRELOAD

It is easy to show from Equation (2) that, if the retainer is progressively tightened so the total preload, P, increases from P1 to P2 while all other parameters remain fixed, the resulting axial contact stress changes by a factor of $(P2/P1)^{1/2}$. A 10-fold increase in preload therefore increases the stress by a factor of 3.162.

5. STRESS VARIATION WITH LENS AND MOUNT MATERIALS

The first and second terms of Equation (8) above apply independently to the two materials used in the lens and the mount. For convenience, that equation can be expressed as:

$$K_2 = K_G + K_M \qquad (14)$$

where $K_G = (1 - \upsilon_G^2)/E_G$ and $K_M = (1 - \upsilon_M^2)/E_M$.

The effects upon stress of changes in each material are considered next. Although lenses are commonly made of glass, crystals or plastic, we limit our considerations here to optical glass materials. Six types of metals used more or less commonly in lens mounts also are considered.

Walker[6] selected 62 basic types of optical glass offered by various manufacturers that "span the most common range of index and dispersion and have the most desirable characteristics in terms of price, bubble content, staining characteristics and resistance to adverse environmental conditions".

The factor K_G was calculated from the above equation for the 68 Schott varieties included in Walker's list. Figure 10 shows, in bar-graph form, how the magnitude of K_G varies for this family of glasses. The sequence is by increasing glass type designation and hence by increasing index of refraction.There is no apparent correlation between K_G and index of refraction. The glasses with the highest (1.190×10^{-7} in.^{2}/lb for F4) and lowest (5.083×10^{-8} in.^{2}/lb for LaSFN30) values of K_G are marked. The ratio of these extreme values is 2.34. Table 1 gives the pertinent mechanical properties of these extreme glasses. Properties data were obtained from the Schott catalog.[7]

Table 2 lists mechanical properties of the 6 types of metals selected for consideration here. The properties data were obtained from Table 3.15 of Ref. 2. K_M was calculated from the above equation and varies from 2.366×10^{-8} in.^{2}/lb (for beryllium) to 1.350×10^{-7} in.^{2}/lb (for magnesium). The ratio of these extreme values is 5.70. Figure 11 shows graphically how K_M varies for these 6 metals.

It should be noted that low values for either K_G or K_M tend to increase lens stress since these factors appear in the denominator of Equation (2).

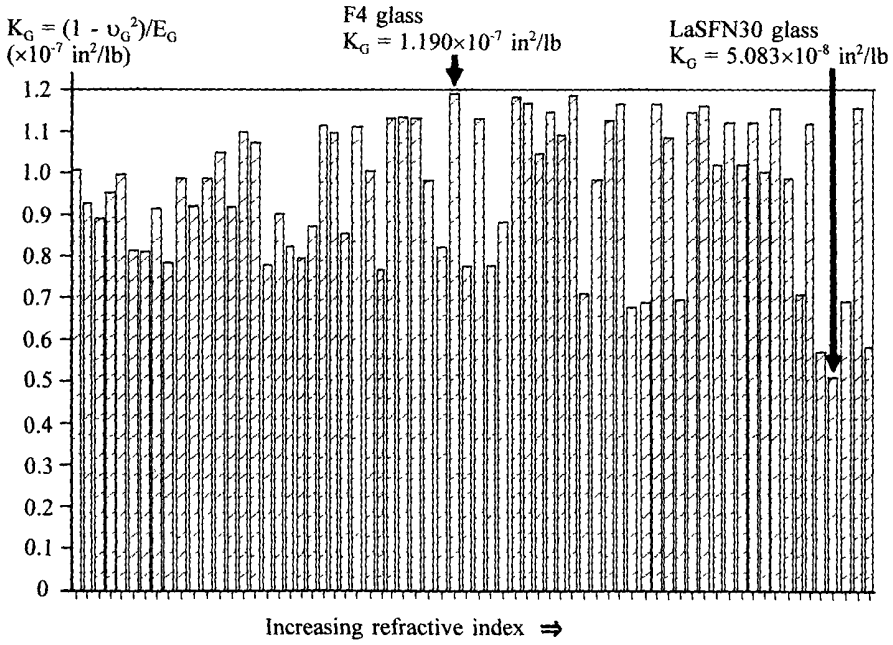

Fig. 10 - Variation of magnitude of K_G for 68 Schott glasses selected by Walker[6]. The left to right sequence is by increasing glass type code and, hence, by refractive index.

Table 1 - Mechanical properties of the Schott glasses included in Walker's[6] list of preferred glass types that have the lowest and highest value for K_G.

Rank	Glass Name	Glass Type	Young's Modulus (E_G) lb/in.^{2}	Poisson's Ratio (υ_G)	$K_G = (1 - \upsilon_G^2)/E_G$ in.^{2}/lb	Thermal expansion Coefficient (α) /°F
1	F4	617366	7.98E+06	0.225	1.190E-07	4.6E-06
2	LaSFN30	803464	1.80E+07	0.293	5.083E-08	3.4E-06

Table 2 - Mechanical properties of some metals used in lens mounts. Rank is by increasing K_M .

Rank	Metal Type	Young's Modulus (E_G) lb/in.^{2}	Poisson's Ratio (υ_G)	$K_G = (1 - \upsilon_G^2)/E_G$ in.^{2}/lb	Thermal expansion Coefficient (α) /°F
1	Be I70A	4.2E+07	0.080	2.366E-08	1.6E-05
2	CRES 416	2.90E+07	0.300	3.138E-08	5.5E-06
3	Invar 36	2.14E+07	0.290	4.28E-08	7.0E-07
4	Ti6Al4V	1.65E+07	0.340	5.36E-08	4.9E-06
5	Al 6061	9.9E+06	0.332	8.988E-08	1.3E-05
6	Mg AZ31B	6.50E+06	0.350	1.350E-07	1.4E-05

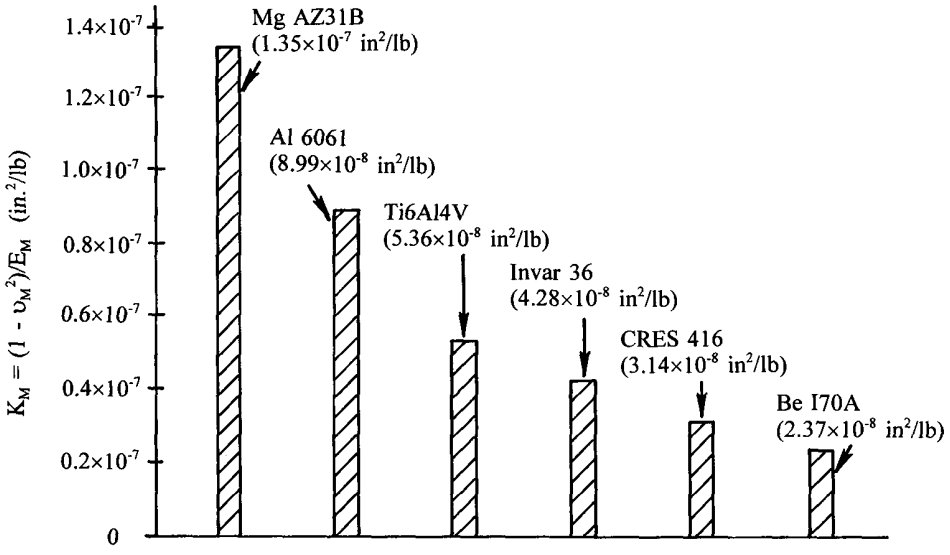

Fig. 11 - Variation of K_M for 6 metals typically used in lens mounts in optical instruments.

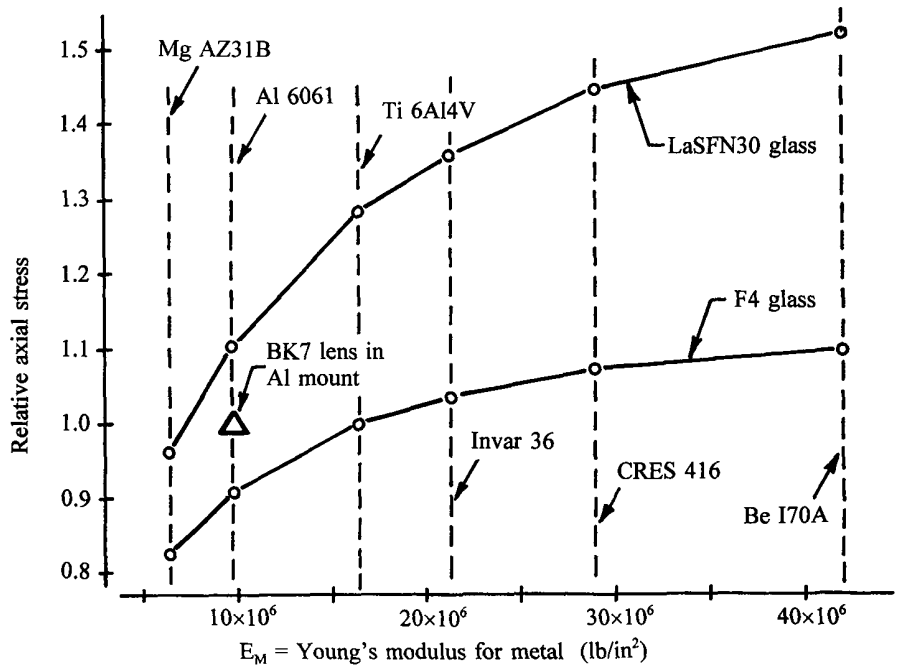

Fig. 12 - Variations of normalized axial stress in lenses made of two types of glass when mounted in different metals.

Analysis of combinations of the metals from Table 2 with the two glasses of Table 1 while keeping preload and interface type constant allowed us to plot typical variations of axial stress with material type. Figure 12 illustrates this. The vertical scale is normalized to the stress level of a BK7 lens in an aluminum mount (see triangle). The horizontal scale is Young's modulus for the metals. The spacings of the vertical dashed lines representing the selected metals give us a sense of the variation of this important parameter from one metal to another. The two curved lines connect discrete points representing particular combinations of glasses and metals. They are not really continuous functions. The fact that the curves diverge towards the right indicates the greater significance of differing glass characteristic K_G for the stiffer metals with small K_M values.

6. TEMPERATURE SENSITIVITY VARIATION WITH LENS AND MOUNT MATERIALS

As stated earlier, lens and mount materials with dissimilar thermal expansion coefficients produce changes in axial preload exerted onto the lens when the temperature changes. Equations (9) through (13) apply.

The relationship between preload change and temperature change (see Equation (9)) is linear for any combination of lens and mount materials. The factor K_3 is the slope of this line; it depends upon geometry of the design as well as the material properties. This is shown graphically in Fig. 13 wherein the behavior of three examples of tangential-interface mount designs for similar equi-convex lens types of different apertures are depicted. All mounts are titanium and all lenses are Schott K4. The designs are defined in Table 3. In Design No. 2, all linear dimensions are scaled up by a factor

of two relative to the baseline (Design No. 1). Similarly, Design No. 3 is scaled up from Design No. 2 by another factor of two.

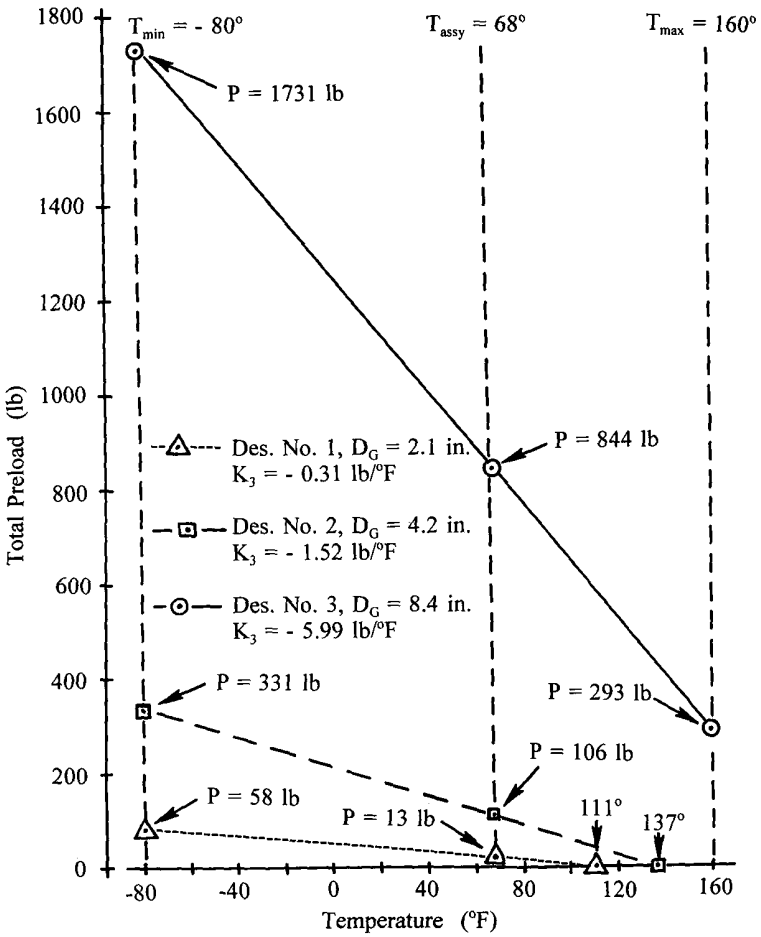

Fig. 13 - Variations of axial preload with temperature for similar equi-convex F4 lenses of different diameters when clamped in titanium mounts with assembly preloads designed to hold the lenses against 300 G accelerations at 68°F.

The preload applied at assembly in each example is that required to just hold the lens' weight against an acceleration of 300 G at 68°F. As may be seen from Table 3, as the temperature rises, this preload decreases. In Design No. 1, the preload goes to zero at 111°F. This is not a serious design defect since the induced axial clearance between the lens and mount at T_{max} is only $(160 - 111)(\alpha_M - \alpha_G)(t_E) = 1\times10^{-6}$ in. In Design No. 2, the preload is released at 137°F and the maximum clearance is again 1×10^{-6} in. In Design No. 3, some preload (293 lbs) still exists at T_{max}.

As the temperature decreases, the preload naturally increases. The worst case total preload and axial stress at T_{min} are 1731 lb and 1029 lb/in.^{2} respectively for Design No. 3. No damage would be expected from this level of stress.

With lens and mount materials having larger disparity of expansion coefficient than existing in these examples, the values of K_3 and the significance of post-assembly temperature changes would be expected to be greater than shown here.

7. SUMMARY

In this paper, we have attempted to show how the mounting stresses developed within an axially clamped lens can be estimated under various conditions as well as how these effects are influenced by changes in design parameters and temperature changes. It should be remembered that the analytical techniques described here are only approximations and that true understanding of the behavior of a given design can be achieved only from more precise analysis or by testing representative hardware.

8. REFERENCES

1. Yoder, Paul R. Jr., "Advanced considerations of the lens-to-mount interface", Proc. SPIE CR43, Optomechanical Design, 305 (1992).

2. Yoder, Paul R. Jr., Chapter 4 in Opto-Mechanical System Design, 2nd Ed., Marcel Dekker, New York (1992).

3. Roark, R. J. , Table XIV in Formulas for Stress and Strain, McGraw-Hill, New York (1954).

4. Delgado, R. F. and Hallinan, M., "Mounting of lens elements", Opt. Eng. 14, S-11 (1975).

5. Yoder, Paul R. Jr., "Axial stresses with toroidal lens-to-mount interfaces", Proc. SPIE 1533, 2 (1991).

6. Walker, B. H., " 'Select' Optical Glasses", The Photonics Design and Applications Handbook, Laurin Publishing Co., Pittsfield, MA, H-356 (1993).

7. Optical Glass Catalog 3111e, Schott Glass Technologies, Inc., Duryea, PA.

Table 3 - Design parameters for three design examples of baseline, 2x and 4x scaled sizes; all represent tangent interfaces on convex lens surfaces.

Design		No. 1	No. 2	No. 3
Lens diam., D_G	(in.)	2.1	4.2	8.4
Ax. thickness, t_A	(in.)	0.117	0.234	0.467
Edge thickness, t_E	(in.)	0.080	0.160	0.320
Radius, $R_1 = - R_2$	(in.)	30.0	60.0	120.0
Mount ID, D_M	(in.)	2.12	4.24	8.48
Mount thickness, t_C	(in.)	0.031	0.062	0.125
Contact height, y	(in.)	1.000	2.000	4.000
Environmental requirements:				
Max. accel., A	(G)	300		
Assy. temp., T_{assy}	(°F)	68		
Max. temp., T_{max}	(°F)	160		
Min. temp., T_{min}	(°F)	-80		
Lens material:		F4		
Young's mod., E_G	(lb/in.^{2})	7.98E06		
Poisson's ratio, υ_G		0.225		
CTE, α_G	(/°F)	4.6E-06		
Mount material:		6061Al		
Young's mod., E_G	(lb/in.^{2})	1.65E07		
Poisson's ratio, υ_G		0.340		
CTE, α_G	(/°F)	4.9E-06		

Table 4 - Evaluation of preloads and mounting stresses for three examples at various temperatures

Design		No. 1	No. 2	No. 3
K_1	(/in.)	1.667E-02	8.333E-03	4.167E-03
K_G	(lb/in.^{2})	1.190E-07		
K_M	(lb/in.^{2})	5.360E-08		
K_2	(lb/in.^{2})	1.726E-07		
A_G	(in.^{2})	0.503	2.011	8.042
A_M	(in.^{2})	0.210	0.838	3.207
K_3	(lb/°F)	-0.306	-1.523	-5.993
Lens wgt., W	(lb)	0.044	0.352	2.813
At assembly:				
P	(lb)	13.20	105.6	843.9
p	(lb/in.)	2.101	8.403	33.58
S_A	(lb/in.^{2})	360	508	718
At T_{max}:				
P	(lb)	0 *	0 *	292.5
p	(lb/in.)	0	0	11.64
S_A	(lb/in.^{2})	0	0	423
At T_{min}:				
P	(lb)	58.5	331	1731
p	(lb/in.)	9.31	26.34	68.87
S_A	(lb/in.^{2})	757	900	1029
* contact is lost at		111°	137°	---
axial clearance at T_{max}		1E-06	1E-06	---